# INVESTIGATING TORUS BIFURCATIONS IN THE FORCED VAN DER POL OSCILLATOR

BERND KRAUSKOPF* AND HINKE M. OSINGA†

**Abstract.** We demonstrate a new algorithm for computing one-dimensional stable and unstable manifolds of (Poincaré) maps that we have implemented in DsTool [1]. As an example we investigate the most complicated sequence of bifurcations in the forced Van der Pol oscillator as the amplitude of the forcing is increased. This bifurcation sequence has recently been used to test algorithms for the computation of invariant tori.

**Key words.** Numerical computations of (un)stable manifolds, Poincaré map, invariant torus, Van der Pol oscillator.

**AMS(MOS) subject classifications.** Primary 58F 65D 34D.

**1. Introduction.** The package DsTool [1] is a well-known and much-used tool for exploring the dynamics of a given dynamical system, which may be given as a vector field or as a map. Furthermore, DsTool allows the user to incorporate user defined algorithms. In this paper we demonstrate a new algorithm for computing one-dimensional unstable manifolds of saddle points of maps, which we implemented such that it operates inside the DsTool environment. Note that DsTool already has a routine for the computation of one-dimensional manifolds of maps: a fixed number of points on the linear eigenspace is iterated a prescribed number of times. This may result in a poor representation of the manifold, or requires the iteration of a great number of points, which is quite time-consuming.

Our alternative method grows the manifolds and adapts the stepsize according to the curvature of the manifold. It is sketched in Section 2; for more details we refer to [10]. Because the algorithm now operates in the DsTool environment, the user can use standard DsTool routines for plotting and for finding periodic points and eigenvectors. The key idea of growing the manifold independently of the dynamics is also behind the algorithm for the computation of two-dimensional unstable manifolds in [9]. A panel in DsTool for the computation of two-dimensional manifolds is work for the future.

As a test example we investigate the forced Van der Pol oscillator; see [6] as general reference. This system has been used in [3] and in [4, 5, 12] to test algorithms for computing normally hyperbolic invariant circles of maps, and normally hyperbolic invariant tori of vector fields, respectively. We fix the parameters in such a way that we are sure to encounter the most complicated sequence of bifurcations as the amplitude of the forcing

*Theoretical Physics, Vrije Universiteit, De Boelelaan 1081, 1081 HV Amsterdam, The Netherlands (berndk@nat.vu.nl)

†The Geometry Center, 400 Lind Hall, 207 Church Street S.E., Minneapolis, MN 55455, U.S.A. (hinke@geom.umn.edu)

is increased. This sequence is interesting in itself, as it corresponds to bifurcations of an invariant torus — an invariant circle for the Poincaré map. Furthermore, the scenario we consider here is one of the test cases in [12]. We illustrate this sequence of bifurcations by representative phase portraits of the Poincaré map with stable and unstable manifolds of a saddle point; see Figs. 3 and 4. Furthermore, we suspend some invariant circles and show the corresponding tori.

**2. The algorithm.** We now sketch the algorithm and its implementation in DsTool [1]. For more details we refer to [10]. The main idea is to grow the manifold with a speed that is determined by the curvature of the manifold. To fix terms, let $f : \mathrm{R}^2 \to \mathrm{R}^2$ be an orientation preserving diffeomorphism with a saddle point $x_0$.

We start with two points, $p_0 = x_0$ and $p_1$ on the linear unstable eigenspace $E^u(x_0)$ at a distance $\delta$ from $x_0$. The algorithm produces a growing list $M = \{p_0, p_1, \ldots, p_N\}$ of points (approximately) on the unstable manifold $W^u(x_0)$. The total number of mesh points $N$ is determined implicitely by the accuracy and the required arclength $l$, both specified by the user. The unstable manifold $W^u(x_0)$ is approximated by the piece-wise linear interpolation of the points in $M$. We denote this continuous approximant by $W^u_{\mathrm{pl}}(x_0)$. During the computation, points are added to $M$, and intervals are added to $W^u_{\mathrm{pl}}(x_0)$.

We now describe a single step of the algorithm, in wich an additional point $p_{k+1}$ is added to $M = \{p_0, p_1, \ldots, p_k\}$. Suppose that we have a good estimate for the distance $\Delta_k$ that we require between $p_k$ and $p_{k+1}$. This distance $\Delta_k$ depends on the curvature of the manifold, and we will explain below how it is determined. We need to find the new point $p_{k+1}$ (approximately) on $W^u(x_0)$ at distance $\Delta_k$ from $p_k$. To this end, we determine the interval $L \in W^u_{\mathrm{pl}}(x_0)$ that is mapped by $f$ to a curve intersecting the circle around $p_k$ with radius $\Delta_k$. To find $L$ we start the search at the preimage of $p_k$ in $W^u_{\mathrm{pl}}(x_0)$. When $L$ is determined we find a point $q \in L$ with

$$(1-\varepsilon)\Delta_k < ||f(q) - p_k|| < (1+\varepsilon)\Delta_k \ .$$

The extra parameter $\varepsilon$ cuts down the number of bisection steps and can be specified by the user.

The point $f(q)$ is a candidate for $p_{k+1}$, but we need to check if the distance $\Delta_k$ was chosen well. We use a method based on the idea in [8] to monitor the curvature. The angle $\alpha_k$ between the points $p_{k-1}$, $p_k$ and $p_{k+1}$ can be estimated by

$$\alpha_k = \frac{||\bar{p} - p_{k-1}||}{||p_k - p_{k-1}||} \ ,$$

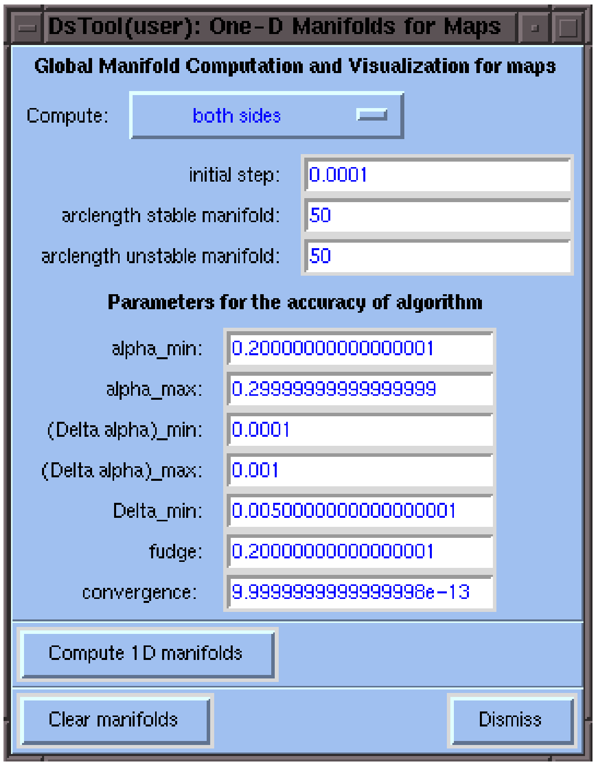


FIG. 1. *The new DsTool window for the computation of one-dimensional stable and unstable manifolds.*

where $\bar{p} = p_k + (p_k - p_{k-1})/||p_k - p_{k-1}||$. The key idea is to check the conditions

$$\begin{array}{rcccl} \alpha_{\min} & < & \alpha_k & < & \alpha_{\max} \\ (\Delta\alpha)_{\min} & < & \Delta_k\alpha_k & < & (\Delta\alpha)_{\max} . \end{array}$$

If $\alpha_k < \alpha_{\max}$ and $\Delta_k\alpha_k < (\Delta\alpha)_{\max}$ the candidate $p_{k+1} = f(q)$ is accepted. If also $\alpha_k < \alpha_{\min}$ and $\Delta_k\alpha_k < (\Delta\alpha)_{\min}$ we set $\Delta_{k+1} = 2\Delta_k$, because the distance $\Delta_k$ was rather small. If the latter is not the case we keep the old distance and simply set $\Delta_{k+1} = \Delta_k$. This finishes the step. In case $\alpha_k > \alpha_{\max}$ or $\Delta_k\alpha_k > (\Delta\alpha)_{\max}$ the point $f(q)$ is not accepted. We then set $\Delta_k = \Delta_k/2$ and repeat the search for $p_{k+1}$ with this smaller $\Delta_k$.

For more details on this adaptation strategy we refer to [10]. The user can specify a minimal value $\Delta_{\min}$. The algorithm changes to iterating points if $\Delta_k < \Delta_{\min}$, which is for example the case when the manifold gets attracted to a fixed point. The user also specifies a minimal distance between consecutive mesh points below which convergence is assumed.

This algorithm can be incorporated in DsTool. Figure 1 shows the control window that allows to specify the parameters of the computation. It is possible to compute both sides of $W^u(x_0)$ separately or together. The first input line sets the initial step $\delta$ along $E^u(x_0)$. Then one specifies the required arclengths of the stable and unstable manifolds. As accuracy parameters one needs to set the curvature parameters $\alpha_{\min}$, $\alpha_{\max}$, $(\Delta\alpha)_{\min}$ and $(\Delta\alpha)_{\max}$, the minimal value $\Delta_{\min}$, the 'fudge factor' $\varepsilon$, and the minimal distance between mesh points as 'convergence' parameter. The values in Fig. 1 are the defaults for these parameters. After a suitable fixed point has been found by standard DsTool routines, the manifolds can be computed by clicking on the 'Compute 1D manifolds' button.

**3. The forced Van der Pol oscillator.** Probably the best known example of a periodically forced system is the forced Van der Pol oscillator

$$\ddot{x} + \alpha(x^2 - 1)\dot{x} + x = \beta \cos \omega t$$

with nonnegative real parameters $\alpha$, $\beta$ and $\omega$. This system models an $RCL$–circuit, and its derivation is, for example, described in [7] for the unforced case $\beta = 0$. The forced Van der Pol oscillator can be written as a three-dimensional vector field with coordinates $(x, y, t) := (x, \dot{x}, \omega t) \in \mathrm{R}^2 \times \mathrm{R}/2\pi\mathrm{Z}$:

$$\left\{ \begin{array}{lcl} \dot{x} & = & y \\ \dot{y} & = & -x - \alpha(x^2 - 1)y + \beta \cos t \\ \dot{t} & = & \omega\ . \end{array} \right. \tag{3.1}$$

We now discuss some properties of (3.1) and refer to [6, 7] as general references. For the unforced system ($\beta = 0$) the third equation decouples, so that the system is governed by the planar $(x, y)$-system. It is not hard to show that this planar system has an attracting limit cycle for $\alpha < 2$, which corresponds to an invariant torus of (3.1). The torus is normally hyperbolic, hence, it persists for small values of $\beta$. We are interested in how this torus deforms as $\beta$ increases and how it bifurcates. To this end, we consider the global Poincaré map $P_{\alpha,\beta,\omega}$, the stroboscopic map of the $2\pi$-periodic forcing term $\beta \cos t$. In order to study the torus we study the bifurcations of the corresponding invariant circle of $P_{\alpha,\beta,\omega}$.

The bifurcation diagram for the forced Van der Pol oscillator has already been studied; see again [6]. Note that (3.1) is equivalent to the system in [6] via the coordinate change $(x, y, t) \mapsto (x, y + \alpha(x^3/3 - x), t/\omega)$. By averaging over the $2\pi$-periodic forcing term, a two-dimensional vector field is obtained in [6] for which the complete bifurcation diagram is given. It is also discussed how this bifurcation diagram relates to the bifurcation diagram of the Poincaré map $P_{\alpha,\beta,\omega}$. Guided by these results, we find the route in parameter space $\alpha = 0.4$, $\omega = 0.893$ and $\beta \geq 0$, which captures the most complicated sequence of bifurcations for the forced Van der Pol oscillator.

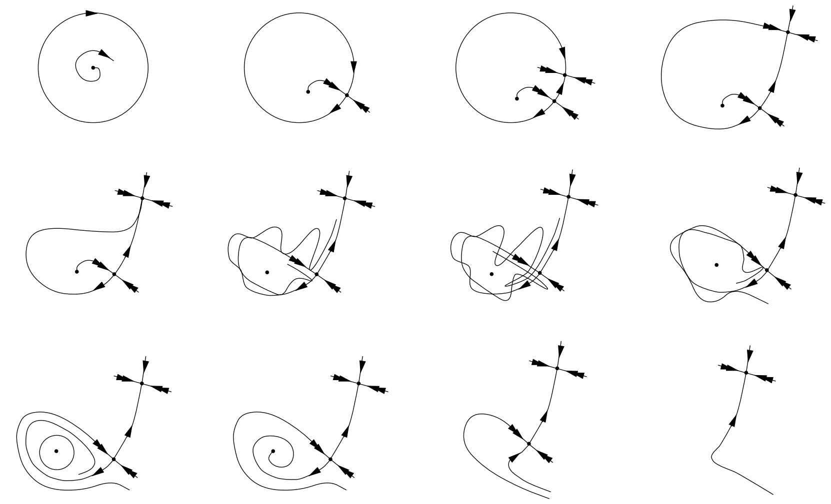

FIG. 2. *Sketch of the most complicated bifurcation sequence of the forced Van der Pol oscillator.*

A sketch of the bifurcation sequence is shown in Fig. 2. The normally hyperbolic invariant circle becomes phase locked in a saddle-node bifurcation on the circle. It then loses its normal hyperbolicity when one side of the unstable manifold of the saddle coincides with the strong stable manifold of the attractor. This is not a bifurcation in the topological sence, and the torus still exists after this event as a continuous object. The torus breaks up in a homoclinic tangle, which is entered and exited via a first and a last homoclinic tangency. Note that for the averaged vector field in [6] there is only a homoclinic connection. This connection becomes a homoclinic tangle when the time-one map of the averaged vector field is perturbed to obtain the Poincaré map. The region with homoclinic tangle in parameter space and the tangle itself in phase space are known to be exponentially small. After the last homoclinic tangency there is an attracting limit cycle, which disappears in a Neimarck-Sacker bifurcation (Hopf bifurcation for maps). Finally, the saddle and the repellor disappear in another saddle-node bifurcation.

**4. Numerical investigations.** In this section we present the numerical computations of the torus bifurcations. The computations are done by using DsTool [1] with the additional routine described in Section 2. The Poincaré map $P_{\alpha,\beta,\omega}$ of the forced Van der Pol oscillator given in (3.1) was explicitely added as a model to DsTool. By this we mean, that we implemented a procedure that numerically computes the Poincaré map of (3.1) by intergration over the forcing period $2\pi$. We used the fourth-order Runge-Kutta method as given in [11] with fixed integration step. The pro-

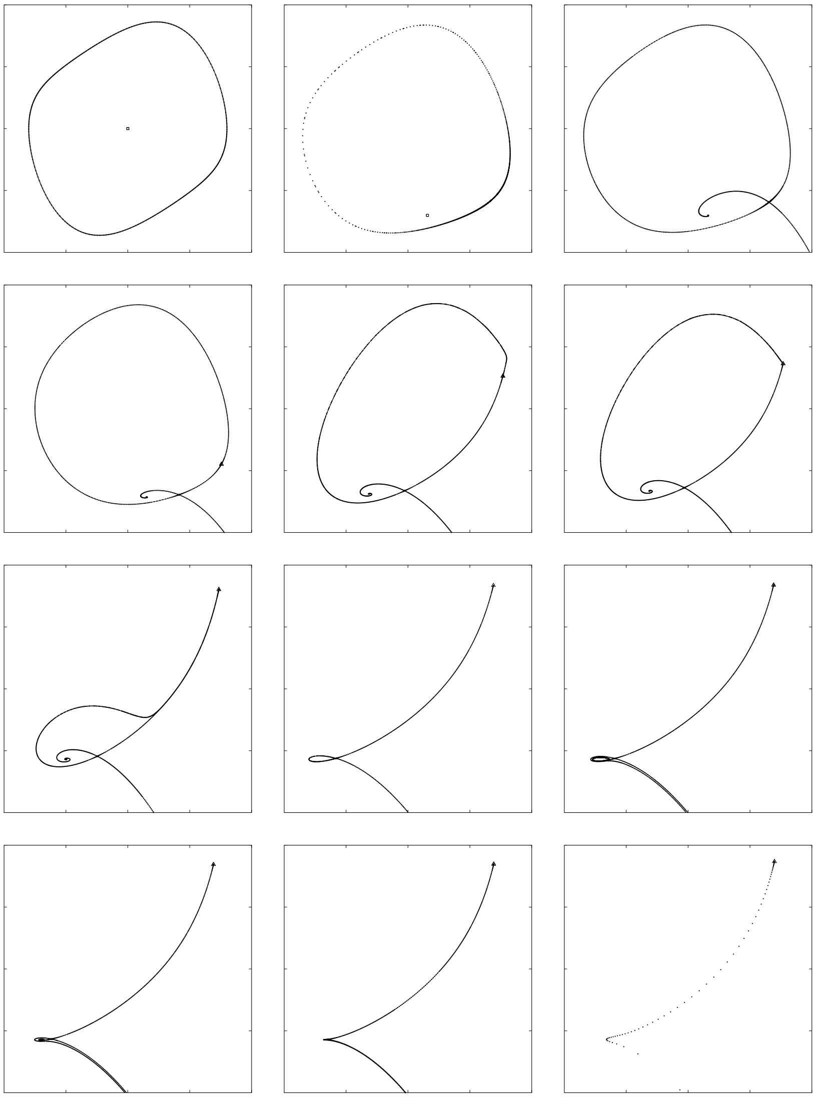

FIG. 3. *Phase portraits of (3.1) for $\alpha = 0.4$, $\omega = 0.893$. From top left to bottom right there is $\beta = 0.0$, $\beta = 0.359$, $\beta = 0.3599$, $\beta = 0.37$, $\beta = 0.374$, $\beta = 0.3740954$, $\beta = 0.375$, $\beta = 0.37601221$, $\beta = 0.3761$, $\beta = 0.37625$, $\beta = 0.376348667$ and $\beta = 0.377$.*

cedure can be controlled by an extra parameter that specifies the number of integration steps on the $[0, 2\pi]$-interval, which was set to 100 throughout our computations.

The main result can be found in Fig. 3 and the enlargments in Fig. 4. They show phase portraits of $P_{\alpha,\beta,\omega}$ for $\alpha = 0.4$, $\omega = 0.893$ and increasing

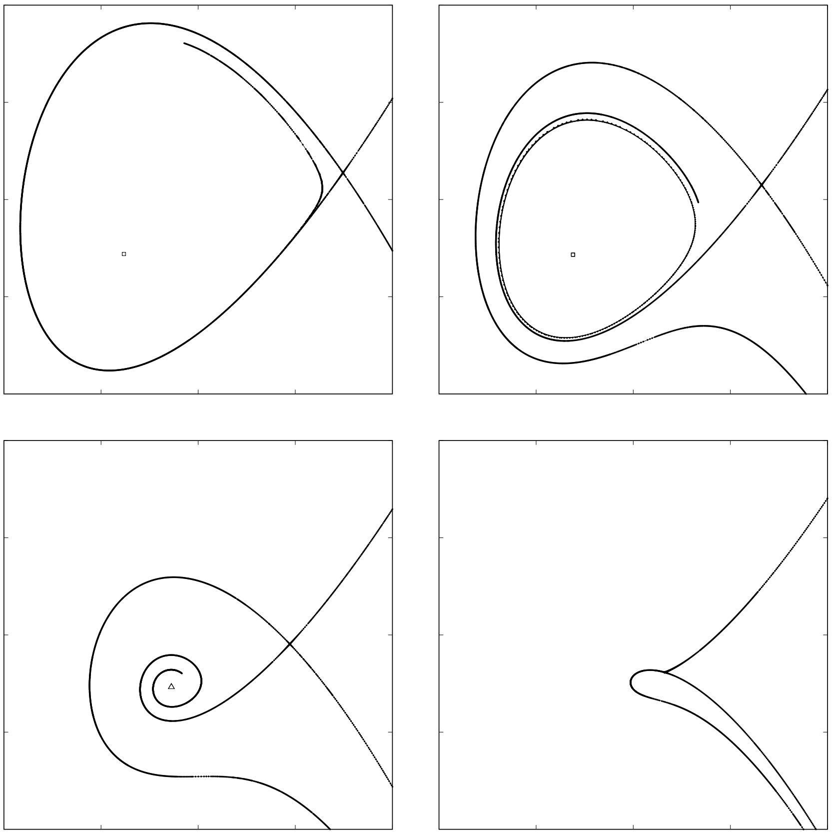

FIG. 4. *Enlargements of phase portraits from Fig. 3. From top left to bottom right there is* $\beta = 0.37601221$*,* $\beta = 0.3761$*,* $\beta = 0.37625$ *and* $\beta = 0.376348667$*.*

$\beta$, and should be compared with Fig. 2. For $\beta \in [0,\ 0.3599)$ there is an invariant circle with periodic motion, with a repellor inside it. For $\beta \approx 0.3599$ a saddle-node bifurcation occurs on the circle, creating a saddle and an attractor. For $\beta \in (0.3599,\ 0.374094)$ the dynamics on the invariant circle is phase locked, but still normally hyperbolic. At $\beta \approx 0.374094$ the flip of the unstable manifold of the saddle with respect to the strong stable manifold of the attractor takes place, in which the torus loses its normal hyperbolicity. It persists as a continuous torus with a cuspidal part for $\beta \in (0.374094,\ 0.37601221)$.

At $\beta \approx 0.37601221$ stable and unstable manifold change their relative positions, see Fig. 4. As we mentioned in Section 3, this change is actually a change through homoclinic tangle, bounded by a first and a last homoclinic tangency. However, even with the full accuracy of DsTool we were not able

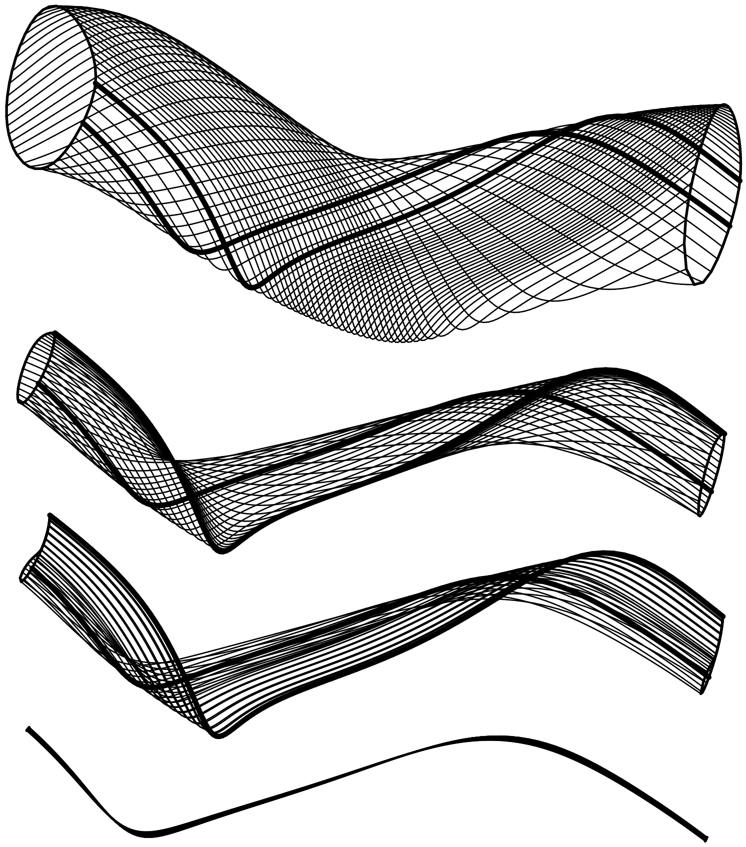

FIG. 5. *Tori of the forced van der Pol oscillator. From top to bottom there is* $\beta = 0.37$, $\beta = 0.3740954$, $\beta = 0.375$ *and* $\beta = 0.3761$.

to find the homoclinic tangle. We conclude that the approximation of $P_{\alpha,\beta,\omega}$ by the averaged vector field is extremely good for the parameter values we chose. The $\beta$-range in which there is tangle, as well as the tangle itself, are so small that they cannot be found with the available accuracy. It is well-known that it is difficult to find transverse intersections of stable and unstable manifolds of maps that admit an approximation by a vector field; see, for example, Figs. 3.8 and 3.16 in [2].

In the homoclinic bifurcation the cuspidal part of the circle got 'cut off', and a new normally hyperbolic invariant circle is born. This circle is indeed a lot smaller than the old continuous one. It exists for $\beta \in (0.37601221,\ 0.376176085)$, and disappears in a Neimarck-Sacker bifurcation at $\beta \approx 0.376176085$. The saddle, the attractor and the repellor

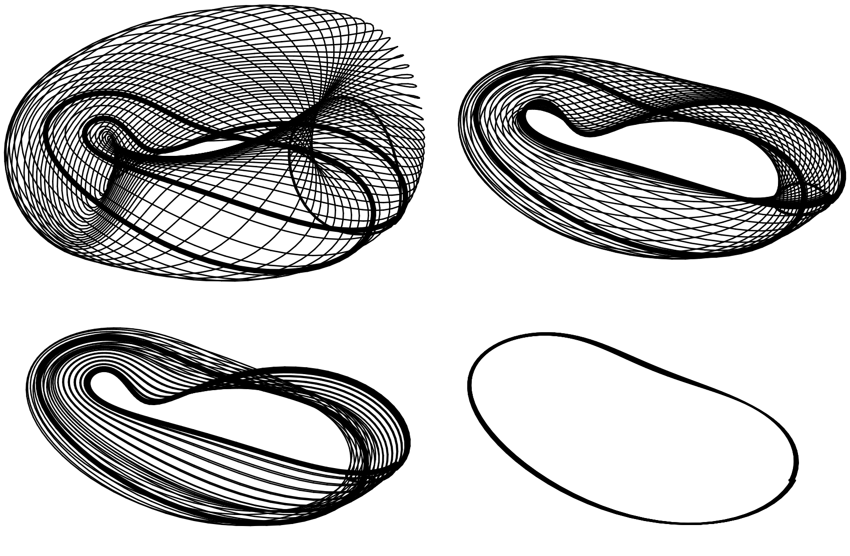

FIG. 6. *The tori of Fig. 5 embedded in* $\mathbb{R}^3$. *From top to bottom there is* $\beta = 0.37$, $\beta = 0.3740954$, $\beta = 0.375$ *and* $\beta = 0.3761$.

keep existing for $\beta \in (0.3761,\ 0.376348667)$. For $\beta \approx 0.376348667$ there is a second saddle-node bifurcation, in which the saddle and the repellor disappear. Note that the shape of the stable and unstable manifolds at the moment of this second saddle-node bifurcation indicates that the parameters are close to a Bogdanov-Takens bifurcation. For $\beta > 0.376348667$ we are left with just the attractor.

To give an impression of the actual tori, we suspended the Poincaré map by integrating a selected number of points, on the invariant circle or on $W^u(x_0)$, over one forcing period. The result is shown in Fig. 5 in the covering space of the phase-space $\mathbb{R}^2 \times \mathbb{R}/2\pi\mathbb{Z}$ of (3.1). The bold curves are the supensions of the saddle point and the attractor, that is, they are two periodic orbits of (3.1), one of saddle type and the other attracting. Figure 6 shows the same tori embedded in $\mathbb{R}^3$. It can clearly be seen how the torus loses its normal hyperbolicity and then has a cuspidal part, which is 'cut off' to produce a much smaller normally hyperbolic torus.

As we mentioned earlier, this bifurcation sequence was used in [12] to test an algorithm for the computation of normally hyperbolic invariant tori of the full three-dimensional system (3.1). As normal hyperbolicity is required, one can only hope to find the tori for $\beta \in (0,\ 0.374094)$ and $\beta \in (0.37601221,\ 0.3761)$ (for our choice of $\alpha = 0.4$ and $\omega = 0.893$ and increasing $\beta$). The cuspidal invariant torus for $\beta \in (0.374094,\ 0.37601221)$ cannot be found with such a method. Note that the interval with the non-normally hyperbolic torus is quite small. It may be possible to 'jump' over this interval if too large steps are taken in the continuation of the normally hyperbolic invariant torus.

We consider the investigation of this bifurcation sequence a successful test of our algorithm inside the DsTool environment. It is a fast way to produce reliable phase portraits of the map under investigation in a short time. By very precise computations we were able to show that the homoclinic tangle is too small to be found with the accuracy of DsTool. We have checked this by using the standard one-dimensional manifold algorithm of DsTool.

**Acknowledgements.** We thank J. Guckenheimer, J. Lorenz and V. Reichelt for helpful discussions. B.K. thanks the Institute for Mathematics and its Applications for its hospitality and for financial support.

## REFERENCES

[1] A. Back, J. Guckenheimer, M.R. Myers, F.J. Wicklin and P.A. Worfolk, *DsTool: Computer assisted exploration of dynamical systems*, Notices Amer. Math. Soc. **39**(4) (1992), pp. 303–309.

[2] C. Baesens, J. Guckenheimer, S. Kim and R.S. MacKay, *Three coupled oscillators: mode-locking, global bifurcations and toroidal chaos*, Physica D **49** (1991), pp. 387–475.

[3] H.W. Broer, H.M. Osinga and G.Vegter, *Algorithms for computing normally hyperbolic invariant manifolds*, Z. angew. Math. Phys. **48** (1997), pp. 480–524.

[4] L. Dieci and J. Lorenz, *Computation of invariant tori by the method of characteristics*, SIAM J. Numer. Anal. **32**(5) (1995), pp. 1436–1474.

[5] , L. Dieci and J. Lorenz, *Lyapunov-type numbers and torus breakdown: Numerical aspects and a case study*, Numer. Algorithms **14**(1–3) (1997), pp. 79–102.

[6] J. Guckenheimer and P. Holmes, *Nonlinear Oscillations, Dynamical Systems, and Bifurcations of Vector Fields*, Springer-Verlag, NY, second printing, 1983.

[7] M.W. Hirsch and S. Smale, *Differential Equations, Dynamical Systems, and Linear Algebra*, Academic Press, Inc., 1974.

[8] D. Hobson, *An efficient method for computing invariant manifolds of planar maps*, J. Comput. Phys. **104**(1) (1993), pp. 14–22.

[9] B. Krauskopf and H.M. Osinga, *Globalizing two-dimensional unstable manifolds of maps*, electronic research report GCG96, The Geometry Center, to appear in Int. J. Bifurcation & Chaos, 1998.
(`http://www.geom.umn.edu/docs/preprints/online/GCG96.html`)

[10] B. Krauskopf and H.M. Osinga, *Growing unstable manifolds of planar maps*, IMA preprint **1517** (1997), submitted to CHAOS.
(`http://www.ima.umn.edu/preprints/OCT97/1517.ps.gz`)

[11] W.H. Press, S.A. Teukolsky, W.T. Vetterling and B.P. Flannery, *Numerical Recipes in C: the Art of Scientific computing*, Cambridge Univ. Press, second edition, 1992.

[12] V. Reichelt, short talk at the IMA workshop "Numerical Methods for Bifurcation Problems", September 1997.
(`http://elc2.igpm.rwth-aachen.de/~reichelt/indexeng.html`)